

## Supplementary material to:

Odhiambo G.O. and Savage M.J. (2009). Surface layer scintillometry for estimating the sensible heat flux component of the surface energy balance. *S. Afr. J. Sci.* **105**, 208–216.

### Monin-Obukhov similarity theory (MOST) and application to surface layer scintillometry

The atmospheric surface layer is also known as the constant flux layer because, under the assumption of steady-state and horizontal homogeneous conditions, the vertical turbulent flux is nearly constant with height, with variations of less than 10%.<sup>35</sup>

Unlike the EC and BREB methods, which do not invoke MOST, empirical MOST relations are used to convert the scintillometer measurements of the  $C_n^2$  and  $l_0$  into  $H$  and  $\tau$ .<sup>33</sup> Validity of MOST and the determination of the effective measurement height therefore dominate the applicability of flux calculation from optically-determined  $C_n^2$  and  $l_0$ .

Dissipation rate of the turbulent kinetic energy  $\varepsilon$  ( $\text{m}^2 \text{s}^{-3}$ ) can be deduced from  $l_0$  and the definition of Kolmogorov<sup>70</sup> scale  $\eta$ :

$$\eta = l_0 \left( \frac{12 \beta_1}{\text{Pr}} \right)^{-3/4} = \left( \frac{\nu^3}{\varepsilon} \right)^{1/4} \quad (1)$$

or

$$\varepsilon = \nu^3 \left( \frac{7.4}{l_0} \right)^4, \quad (2)$$

where  $\beta_1$  is the Obukhov-Corrsin constant (= 0.86), Pr the Prandtl number (= 0.72) and  $\nu$  the kinematic viscosity of air ( $\text{m}^2 \text{s}^{-1}$ ):<sup>66</sup>

$$\nu = [1.718 + 0.0049(T - 273.15)] \times 10^{-5} / \rho, \quad (3)$$

where  $T$  is the air temperature (K) and  $\rho$  the density of air ( $\text{kg m}^{-3}$ ).

The application of MOST to surface layer scintillometer measurements adopted by Thiermann and Grassl<sup>10</sup> is followed. A simultaneous optically-measured inner scale length  $l_0$  is related to the dissipation rate of turbulent kinetic energy  $\varepsilon$  and one assumes that  $\varepsilon$  obeys MOST. A fixed  $C_T^2$  and  $l_0$  then correspond to a set of values for  $H$  and  $\tau$ . According to MOST, for a constant flux, the structure of turbulence is determined by the following scaling parameters (Table 1):<sup>30</sup>

$$u_* = \sqrt{\tau / \rho} \quad (4)$$

$$T_* = \frac{H}{\rho c_p u_*}, \quad (5)$$

where  $c_p$  is the specific heat capacity of air at constant pressure ( $\text{J kg}^{-1} \text{K}^{-1}$ ).

According to MOST,  $C_T^2$  and  $\varepsilon$  are made dimensionless by respectively scaling them with the temperature scale  $T_*$  and friction velocity  $u_*$ , and are universal functions of the stability parameter  $\zeta = (z-d)/L$ , with the Obukhov length  $L$  defined by:

$$L = -\frac{T \rho c_p}{k g H} \cdot u_*^3, \quad (6)$$

where  $k$  is the von Kármán constant (0.41) and  $g$  is the acceleration due to gravity ( $9.81 \text{ m s}^{-2}$ ).

From MOST:

$$f(\zeta) = \frac{C_T^2 (z-d)^{2/3}}{T_*^2} \quad (7)$$

and

$$g(\zeta) = \frac{\varepsilon k (z-d)}{u_*^3}. \quad (8)$$

Various forms for the stability functions,  $f(\zeta)$  and  $g(\zeta)$ , have been proposed: Thiermann and Grassl<sup>10</sup>, Hill *et al.*<sup>23</sup>, Wyngaard<sup>38</sup>, de Bruin *et al.*<sup>71</sup> and others. The functions used for stable and unstable conditions, as proposed by Thiermann and Grassl<sup>10</sup> and which were used to derive  $H$  by the Scintec<sup>66</sup> SLSRUN software developed for the SLS used, were found adequate.<sup>4</sup>

Thiermann and Grassl<sup>10</sup> give the following semi-empirical expressions for  $f(\zeta)$  and  $g(\zeta)$ : for  $\zeta > 0$  (stable condition)

$$f(\zeta) = C_T^2 (z-d)^{2/3} T_*^{-2} = 4\beta_1 (1-7\zeta + 20\zeta^2)^{-1/3} \quad (9)$$

and

$$g(\zeta) = \varepsilon k (z-d) u_*^{-3} = (1-4\zeta + 16\zeta^2)^{-1/2} \quad (10)$$

and for  $\zeta < 0$  (unstable condition)

$$f(\zeta) = C_T^2 (z-d)^{2/3} T_*^{-2} = 4\beta_1 (1-7\zeta + 75\zeta^2)^{-1/3} \quad (11)$$

$$g(\zeta) = \varepsilon k (z-d) u_*^{-3} = (1-3\zeta)^{-1} - \zeta, \quad (12)$$

where  $\beta_1 = 0.86$  is the Obukhov-Corrsin constant.

Hill *et al.*,<sup>23</sup> on the other hand, proposed that for unstable atmospheric conditions for which  $\zeta < 0$ :

$$f(\zeta) = C_T^2 (z-d)^{2/3} T_*^{-2} = 8.1(1+15\zeta)^{-1/3}. \quad (13)$$

Equations 9 and 10 for stable conditions and Equations 11 and 12 for unstable conditions can be solved for  $H$  and  $\tau$  using a numerical iterative scheme to obtain  $u_*$  and  $T_*$  using the definition of  $L$  (Equation 6). Sensible heat flux  $H$  and momentum flux  $\tau$  are finally obtained from Equations 4 and 5.

### Scintillometry and the role of the refractive index structure constant

The graph of the refractive index spectrum is shown in Fig. 1<sup>72</sup>. According to Kolmogorov<sup>70</sup>, in the inertial sub-range, energy neither enters the system nor is dissipated. It is merely transferred at rate  $\varepsilon$  where  $\varepsilon$  is the dissipation rate of turbulent kinetic energy ( $\text{m}^2 \text{s}^{-3}$ ) (Table 1) from smaller wave numbers to larger

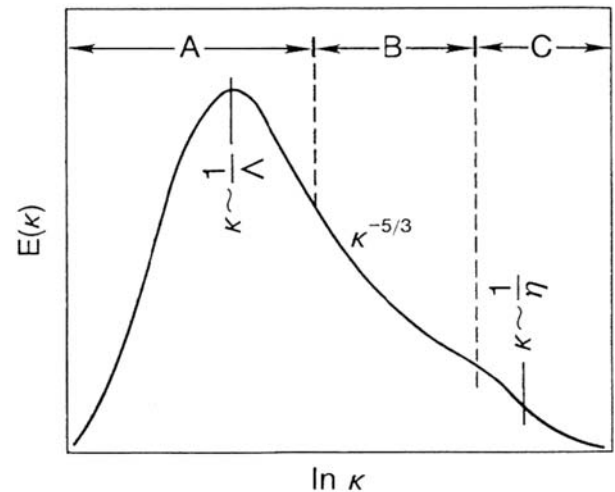


**Fig. 1.** The energy spectrum  $E(k)$  associated with turbulence for a range of wave numbers  $k$  for the various boundary layer flows (taken from Kaimal and Finnigan<sup>72</sup>): **A** corresponds to regions of energy production, **B** to the inertial sub-range of turbulence and **C** to the dissipation range where kinetic energy is converted to internal energy acting to raise the temperature of the fluid. The integral length scale of turbulence is denoted  $\Lambda$  and  $\eta$  denotes the Kolmogorov<sup>70</sup> microscale of length.

**Table 1.** Summary of meteorological parameters estimated or required by the various measurement methods and MOST.

Parameter	Symbol (unit)	Description
Refractive index structure parameter	$C_n^2$ ( $\text{m}^{-2/3}$ )	Spatial statistics used as a measure of the path-averaged strength of refractive turbulence, or simply a measure of the fluctuations in refractive index of air caused mainly by air temperature variations.
Momentum flux density	$\tau$ (Pa)	The turbulent horizontal wind stress in the surface boundary layer.
Bowen ratio	$\beta$ (no unit)	The ratio of sensible heat flux to that of latent energy flux.
Structure function parameter of temperature	$C_T^2$ ( $\text{K}^2 \text{m}^{-2/3}$ )	A measure of the structure of air temperature fluctuations (determined from $C_n^2$ ).
Dissipation rate of turbulent kinetic energy	$\varepsilon$ ( $\text{m}^2 \text{s}^{-3}$ )	Refers to the rate of change in turbulent kinetic energy (TKE) per unit mass of fluid, due to viscous effects.
Fresnel zone	$F$ (m)	$F = \sqrt{\lambda \times L_{\text{beam}}}$ , where $\lambda$ is the wavelength of the transmitter beam and $L_{\text{beam}}$ the beam path length. The most optically-active eddies have sizes of the order of the Fresnel zone.
Inner scale length	$l_0$ (mm)	The smallest diameter of the occurring eddies.
Friction velocity	$u_*$ ( $\text{m s}^{-1}$ )	A basic wind speed scaling parameter equal to the square root of $\tau/\rho$ where $\rho$ is the air density.
Obukhov length	$L$ (m)	The height above the zero-plane displacement height $d$ at which free convection dominates over forced convection.
Zero-plane displacement height	$d$ (m)	A height scale in turbulent flow over roughness elements such as vegetation above the ground at which zero wind speed is achieved as a result of the flow obstacles. It is generally approximated as 2/3 of the average height of the obstacles. The displacement height represents the mean height where momentum is absorbed by the canopy.
Temperature scale of turbulence	$T_*$ (K)	A term for the temperature that an air parcel at a height would potentially have if brought adiabatically (i.e. without thermal contact with the surrounding air) to a given height, i.e. the effective temperature of an air parcel after removing the heat of the parcel associated solely with compression.

**Table 2.** Meteorological parameters determined for selected different methods.

Method used for determination of meteorological parameter	Meteorological parameters						
	$H$	$u_*$	$\varepsilon$	$\tau$	$LE$ residual = $R_{\text{net}} - H - S$	$LE$	$\text{CO}_2$ flux ( $F_c$ )
LAS or XLAS	✓	–	–	–	+	–	–
SLS or multi-beam LAS	✓	✓	✓	✓	+	–	–
1-Dimensional EC	✓	–	–	–	+	–	–
3-Dimensional EC	✓	✓	–	✓	+	–	–
$\text{CO}_2$ sensor and 3-D sonic (EC)	✓	✓	–	✓	–	–	✓
$\text{H}_2\text{O}$ sensor and 3-D sonic (EC)	✓	✓	–	✓	+	✓	–
BR	✓	–	–	–	✓	✓	✓
SR (high frequency air temperature measurements)	✓	–	–	–	+	–	–
SR (high frequency specific humidity measurements)	–	–	–	–	–	✓	–

✓, Meteorological parameter that can be measured using the method.

–, Meteorological parameter that cannot be measured or determined using the method.

+, Meteorological parameter that can be estimated if net irradiance  $R_{\text{net}}$  and soil heat flux  $S$  are known.

wave numbers, where it is dissipated. As a result, the three-dimensional spectral density function,  $\Phi_n(\kappa)$ , where  $\kappa$  is the wave number  $\kappa = 2\pi/l$  associated with the spectrum of eddies of size  $l$ , would depend on the viscous dissipation rate  $\varepsilon$  and the turbulent spatial wave number  $\kappa$  only.

Kolmogorov's first hypothesis<sup>70,72</sup> applies in the range determined by the inequality  $l_0 \ll 1 \text{ m} < \mu$  (called the equilibrium range), where  $\mu$  is called the Kolmogorov microscale (Fig. 1). The Kolmogorov microscale defines the size of eddies dissipating the kinetic energy. The second hypothesis is for sufficiently large Reynolds numbers. The sub-range defined by  $\eta < 1 \text{ m} \ll \Lambda$ , is called the inertial sub-range, where  $\Lambda$  is the outer scale length and is approximately equal to the scintillometer measurement height and  $\eta$  is the Taylor microscale (which marks where the viscous effect becomes significant) and is dominated by inertial forces whose actions redistribute the energy across the turbulent spectrum (Fig. 1).

### Scintillometry theory and determination of $H$

The energy spectrum of turbulence (Fig. 1), representing the scale of turbulence from the so-called energy-containing range

through to the inertial sub-range of turbulence to the dissipation range,<sup>73</sup> may be defined through the use of a wave number for turbulence. The turbulent wave number  $\kappa$  ( $\text{m}^{-1}$ ) range is defined by the corresponding range in eddy size values experienced in the atmosphere with the spectrum of wave numbers occurring due to the numerous eddies of variable size.<sup>73</sup> These eddy sizes are indicative of the turbulence regime of the atmosphere and may impact on the transmission of electromagnetic radiation.

The variance of the natural logarithm of the intensity incident at the receiver is related to  $C_n^2$  defined as:<sup>9</sup>

$$C_n^2 = \frac{(n(r_1) - n(r_2))^2}{r_{12}^{3/2}} \quad (14)$$

where  $n(r)$  is the refractive index at location  $r$  and  $r_{12}$  (m) is a distance lying between two length scales  $r_1$  and  $r_2$  characteristic of the turbulence.<sup>74</sup> The changes in the refractive index of air caused by air temperature fluctuations are usually random functions in both time and space. Thus, turbulence intensity of the refractive index of air  $n(r, t)$  can only be determined by the average of certain quantities, such as  $C_n^2$ . Assuming the random

process generating the changes in refractive index is isotropic, then  $C_n^2(r) = C_n^2 \cdot |r|^{28.75}$

The distance between the transmitter and the receiver can range from tens to thousands of metres depending on the type of instrument. Different types of radiation sources can be used. The beam wavelength for the different scintillometer types is also different, with the LAS and XLAS having a beam wavelength of 930 nm, within 5 nm. The displaced-beam surface layer scintillometer, the SLS, emits two parallel and differently polarised laser beams with the separating distance,  $d_{SLS}$ . The commercial SLS unit, the SLS40-A uses a class 3a type laser at a wavelength  $\lambda$  of 670 nm (which is similar to that of an ordinary laser pointer), a beam displacement distance,  $d_{SLS}$  of 2.7 mm and a detector diameter,  $D_{SLS}$  of 2.5 mm. With this instrument the beam of one source is split into two parallel, displaced beams with orthogonal polarisations. By determining both the variances of the logarithm of the amplitude of the two beams,  $\sigma_1^2$  and  $\sigma_2^2$ , and the covariance of the two beams,  $\sigma_{12}^2$ ,  $l_0$  and  $C_n^2$  can be obtained.<sup>66</sup> At the receiver, usually located 50 m to 250 m away from the transmitter, the two beams reach two separate detectors. The SLS set up is shown (Fig. 2) with a close-up of the transmitter, receiver, junction box and signal processing unit (Fig. 3).

The covariance of the logarithm of the amplitude of the received radiation is given by:<sup>10</sup>

$$\sigma_{12}^2 = 4\pi^2 K^2 \int_{r=0}^{L_{beam}} \int_{\kappa=0}^{\infty} \kappa \Phi_n(\kappa) J_0(\kappa d_{SLS}) \cdot \sin^2 \left[ \frac{\kappa^2 \cdot r \cdot (L_{beam} - r)}{2KL_{beam}} \right] \cdot \left[ \frac{4J_1^2(\kappa D_{SLS} r / 2L_{beam})}{(\kappa D_{SLS} r / 2L_{beam})^2} \right] dk dr \quad (15)$$

Equation 15 is valid for  $\sigma_{12}^2 < 0.3$ , corresponding to weak scattering. If the scattering is not weak, then the measured  $\sigma_{12}^2$  is less than that determined from Equation 15 and saturation is said to occur.<sup>76</sup> Due to this fact, the maximum path length for the SLS is usually limited to 250 m. To overcome the saturation problem, which limits the SLS measurements to a beam path distance of 250 m, the beam path length should be decreased or beam height position increased.<sup>3,60</sup> Otherwise a LAS would be

the option for obtaining  $H$  over longer path lengths, e.g. 5 km to 10 km.<sup>77</sup>

The functional dependence of the covariance  $\sigma_{12}^2$  in Equation 15 includes two wave numbers – the optical wave number  $K$  ( $m^{-1}$ ) for the SLS beam, where  $K = 2\pi/\lambda$ , and where  $\lambda = 670$  nm for the SLS and wave number defined as  $\kappa = 2\pi/l$ , corresponding to the spectrum of eddy sizes that the beam encounters where  $l$  is eddy size. The functional dependence of Equation 15 also includes the function  $\Phi_n(\kappa)$  corresponding to the three-dimensional spectrum of refractive index inhomogeneities caused by the interaction of changes in air temperature with refractive index, SLS beam displacement distance  $d_{SLS}$ , two Bessel functions  $J_0$  and  $J_1$  of the first kind,  $r$  the distance along the beam measured from the transmitter with  $L_{beam}$  corresponding to the beam path length, and  $D_{SLS}$  the aperture diameter of the scintillometer detectors. As presented by Lawrence and Strohbehn<sup>78</sup> and pointed out by Thiermann and Grassl<sup>10</sup>, substituting  $d_{SLS} = 0$  m corresponding to a single beam into Equation 15, provides the expression for the variances  $\sigma_1^2$  and  $\sigma_2^2$  at each of the single detector pairs.

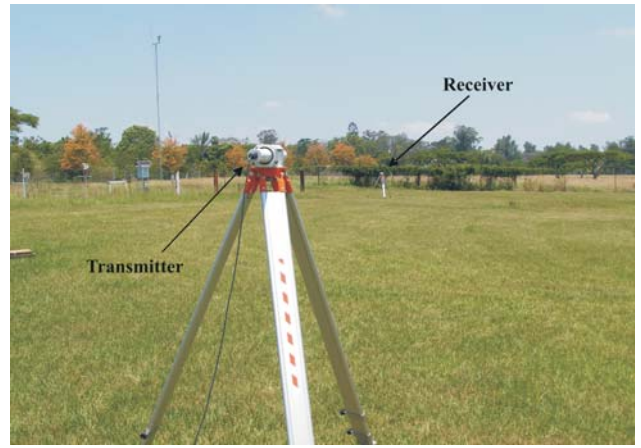


Fig. 2. The surface layer scintillometer set up showing the transmitter and receiver as indicated.

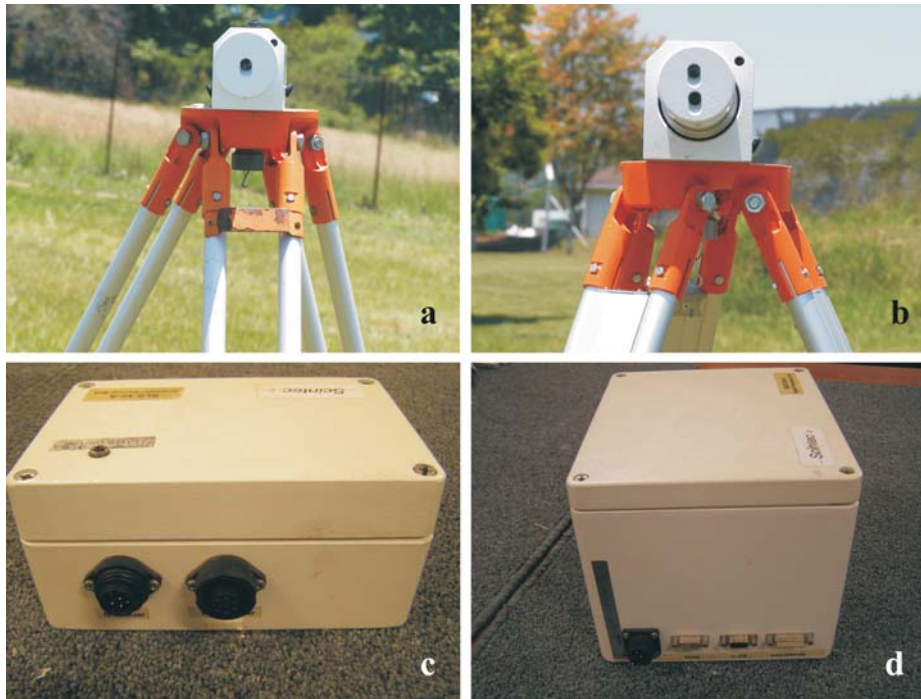


Fig. 3. The SLS (a) transmitter, (b) receiver, (c) switch box and (d) signal processing unit.